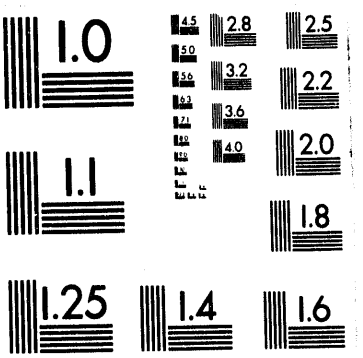
1.0
1.1
1.25
1.4
1.6
1.8
2.0
2.2
2.5
2.8
3.2
3.6
4.0
4.5
5.0

1 of 1

ANL/RA/CP--80543
Conf-940407--9

# BOWING-REACTIVITY TRENDS IN EBR-II ASSUMING ZERO-SWELLING DUCTS*

D. Meneghetti
Argonne National Laboratory
Argonne, IL 60439, U.S.A.

For Presentation at the
1994 Reactor Physics Topical Meeting
Knoxville, Tennessee
April 11-14, 1994



## DISCLAIMER



*Work supported by the U.S.Department of Energy, Nuclear Energy Programs Under Contract W-31-109-ENG-38.

# BOWING-REACTIVITY TRENDS IN EBR-II ASSUMING ZERO-SWELLING DUCTS*

D. Meneghetti

Argonne National Laboratory, Argonne, IL 60439, USA, (708) 252-6712

KEYWORDS: Bowing, Reactivity, EBR-II

## ABSTRACT

Predicted trends of duct-bowing reactivities for the Experimental Breeder Reactor II (EBR-II) are correlated with predicted row-wise duct deflections assuming use of idealized zero-void-swelling subassembly ducts. These assume no irradiation induced swellings of ducts but include estimates of the effects of irradiation-creep relaxation of thermally induced bowing stresses. The results illustrate the manners in which at-power creeps may affect subsequent duct deflections at zero power and thereby the trends of the bowing component of a subsequent power reactivity decrement.

## INTRODUCTION

Trends in duct-bowing reactivities and comparisons with measurement-deduced reactivities for the Experimental Breeder Reactor II (EBR-II) have been reported[1] for subassembly ducts of the 304 type stainless steel which can undergo significant irradiation-induced void-swellings. Considerations of possible use of small-void-swelling steel ducts have now led to analogous calculations for predicted trends in bowing reactivities assuming instead idealized zero-void-swelling irradiation characteristic. These assume no irradiation induced swelling of ducts but include estimates of the effects of irradiation-creep relaxation of thermally induced bowing stresses. Other irradiation and/or temperature dependent parameters used in the previous study are retained. The calculated reactivities are the bowing components of the power reactivity decrements (PRDs). (The PRD at a power is here the negative of the reactivity required to bring the reactor from zero power, hot critical, to that power.)

Trends in bowing component because of duct distortions resulting from irradiation creep are illustrated by a series of simple calculational simulations for a seven-rowed and a six-rowed core size. The larger core is radially reflected by approximately three rows of steel reflector subassemblies. The smaller core is radially reflected by four rows of steel reflector subassemblies. Approximately five rows of depleted-uranium type subassemblies surround these reflectors. Although the subassembly powers, flows and compositions of runs 99A and 122A, respectively, are the bases of these analyses the results are not specific for these runs. The subassemblies also are assumed to be neither moved nor rotated. The results illustrate the manners in which at-power creep may affect subsequent duct distortions at zero power and thereby the trends of the bowing component of a subsequent PRD.

*Work supported by the U.S.Department of Energy, Nuclear Energy Programs Under Contract W-31-109-ENG-38.

Duct deflections at zero power (aside from the effects of the inevitable physical interventions of subassembly insertions, relocations, removals, and rotations) would be primarily from the residual deflections resulting from irradiation-enhanced creep because of the zero void swelling assumption. Since thermal bowing which occurs upon ascent to power results from temperature differences between opposite sides of a duct it is not retained at a subsequent zero power except when the at-power restraint stresses undergo relaxation. The zero power bow can then exhibit a residual deflection in an opposite direction.

## DUCT GEOMETRY

The EBR-II reactor consists of essentially 15 concentric rows of subassemblies having stainless-steel hexagonal ducts. The ducts are 2.29 in. (58.2 mm) wide across flats and 65.8 in. (1670 mm) in length from the supporting grid plate to the top of the hexagonal duct. The 13.5 in. (343 mm) core height is axially centered at 31.3 in. (795 mm) from the duct bottoms. Approximately 1.5 in. (38 mm) above the core centerline the duct faces are dimpled outward 0.014 in. (0.36 mm) to form spacer buttons which have nominal separations of 0.002 in. (0.051 mm) between facing buttons at zero power for unirradiated ducts. A cylindrical lower adapter, which provides inlet orifices for the sodium coolant, protrudes downward into the lower grid structure. The lower structure supports the subassembly and limits its lateral pivoting. The subassembly centerline separations are 2.320 in. (58.9 mm) with unirradiated ducts with separations between adjacent duct faces of 0.030 in. (0.76 mm). Separation of unirradiated ducts at tops of adjacent ducts is 0.027 in. (0.686 mm). The tops of the outermost ducts are limited in outward motions by a restraining ring positioned about 0.030 in. (0.76 mm) outward from the duct tops. This allows for some free bowing at the subassembly tops. Furthermore, this freestanding restraint system does not maintain tightness at the spacer button elevation by external restraint.

## METHOD

The bowing calculations use a modified version[2] of the BOW-V code[3] which takes into account intrarow subassembly interactions at the duct button level, as well as the usual interrow interactions, and can accept initial row-wise radial distortions for zero power inputs. The temperature inputs are obtained by the EBRDUCT code[1] which was developed specifically for use in these studies of trends in EBR-II duct bowings.

The row-wise unrestrained radial distortions of ducts resulting from fast-fluence enhanced creep of at-power restrained ducts are estimated by a modification of the method described in reference 1: Starting at zero power with undistorted ducts a thermal bowing calculation is made. From this is obtained the difference, $\Delta v_t$, between the at-power free thermal deflection, $v_{tf}$, and the at-power restrained thermal deflection, $v_{tr}$, i.e., $\Delta v_t = v_{tf} - v_{tr}$. This axially dependent difference is next adjusted because of the relative lesser fast neutron flux, and hence creep, in axial regions below and above core and in radially corresponding axial levels lateral thereto. For simplicity below core level the difference is taken to be zero; from axial levels of core bottom to core top the deflection difference $\Delta v_t$ is reduced by its value at level of the core bottom to obtain $\Delta v_t^*$ in this axial region; and at axial levels above core this difference is a linear extrapolation of the adjusted value and slope at the core top level. The creep modified free-deflection (used to obtain the zero-power row-interactive restrained distortion in a PRD bowing calculation) assuming complete creep is then approximated by $v^*_{to} = - \Delta v_t^*$ for the row. To approximate the effects of lesser amounts of creep upon the trends in the bowing component of the PRD the term $\Delta v^*_t$ is simply reduced by assumed f-factors, less than unity, for the rows. The analogous relation used for the applicable button-to-button dimension across a subassembly row is $d^*_{to} = d_o - \Delta d_t$ where $\Delta d_t = d_{tf} - d_{tr}$. For lesser creep the latter expression is reduced by the f-factor.

## TEMPERATURES

Listed in Tables 1 and 2 are the intrarow averages of the radially effective values of $\Delta T$ at a few axial levels for runs 99A and 122A respectively. Listed are also the intrarow averaged values of the duct temperatures, $\bar{T}$, above inlet temperature at the button level. (Results are for an assumed power of 60.0 MWt and total intrasubassembly (and intrarod) coolant flow of 8080 gpm (0.510 $m^3 s^{-1}$) of 800°F (427°C) Na; i.e. a discharge of about 8500 gpm (0.536 $m^3 s^{-1}$) from the primary pumps and a total flow through the reactor including the leakage paths of about 8190 gpm (0.517 $m^3 s^{-1}$).)

Table 1. Intra-Row-Average Effective-$\Delta T$ Radially-Across Subassembly-Ducts for Run 99A

| Axial Location | $\Delta T^a$ in °F for Row | | | | | | | | | | | | | | |
|---|---|---|---|---|---|---|---|---|---|---|---|---|---|---|---|
| | 1 | 2 | 3 | 4 | 5 | 6 | 7 | 8 | 9 | 10 | 11 | 12 | 13 | 14 | 15 |
| Clad Top[b] | 0 | -31 | -6 | -15 | -30 | +19 | +38 | -8 | -10 | -32 | +15 | +76 | +62 | +31 | +13 |
| Core Top | 0 | -15 | -8 | -8 | -20 | +14 | +21 | -8 | +2 | -28 | +17 | +58 | +46 | +23 | +9 |
| Core Midplane | 0 | -6 | -4 | -5 | -10 | +7 | +5 | -17 | -1 | -22 | +12 | +39 | +31 | +15 | +6 |
| Core Bottom | 0 | 0 | 0 | -2 | 0 | +1 | -10 | -24 | -6 | -14 | +6 | +20 | +17 | +8 | +4 |
| $\bar{T}^c$ at Midplane | 49 | 45 | 64 | 64 | 86 | 86 | 73 | 89 | 106 | 100 | 121 | 92 | 58 | 36 | 27 |

a. Positive sign indicates duct temperature larger on side closer to core centerline. (Divide by 1.8 for °C)
b. About 13in (33cm) above core-top level. c. Above 700 °F inlet. (371°C)

Table 2. Intra-Row-Average Effective-$\Delta T$ Radially-Across Subassembly-Ducts for Run 122A

| Axial Location | $\Delta T^a$ in °F for Row | | | | | | | | | | | | | | |
|---|---|---|---|---|---|---|---|---|---|---|---|---|---|---|---|
| | 1 | 2 | 3 | 4 | 5 | 6 | 7 | 8 | 9 | 10 | 11 | 12 | 13 | 14 | 15 |
| Clad Top[b] | 0 | +14 | -32 | -17 | -20 | +21 | +110 | -20 | -23 | -28 | +3 | +31 | +62 | +33 | +9 |
| Core Top | 0 | +9 | -18 | -13 | -12 | +7 | +74 | -7 | -12 | -22 | +5 | +25 | +46 | +25 | +7 |
| Core Midplane | 0 | +4 | -8 | -10 | -5 | +8 | +30 | -9 | -10 | -16 | +4 | +17 | +31 | +17 | +4 |
| Core Bottom | 0 | 0 | 0 | -3 | +1 | +1 | -10 | -11 | -9 | -10 | +2 | +8 | +17 | +9 | +2 |
| $\bar{T}^c$ at Midplane | 56 | 54 | 50 | 74 | 89 | 90 | 64 | 61 | 76 | 80 | 91 | 89 | 60 | 37 | 28 |

a. Positive sign indicates duct temperature larger on side closer to core centerline. (Divide by 1.8 for °C)
b. About 13in (33cm) above core-top level. c. Above 700 °F inlet. (371°C)

It is noted that the outer row of core (row 7 for run 99A and row 6 for run 122A) would tend to deflect outward; whereas, the first row of reflector (row 8 for run 99A and row 7 for run 122A) would tend to deflect inward for the larger core and outward for the smaller core. For both cores the reflector row 10 tends to deflect inward and the blanket rows 11-15 tend to deflect outward. The much lesser outward deflecting trends of the blanket row 11 in run 122A is due to the large number of high-flow row 11 blanket subassemblies in run 122A.

It is also noted that the magnitude of the temperature differentials of the first row of reflector (row 7) of run 122A is large; whereas, the magnitude of the negative values for the first row of reflector (row 8) of run 99A is small. This indicates that with seven-rowed cores the unrestrained deflection direction of the first reflector row would be very sensitive to values of power-to-flow ratios of the reflector subassemblies. Because powers and flows of reflector subassemblies are small, small incremental changes of reflector powers and/or flows could lead to substantial changes in the ratios of power-to-flow, in the intersubassembly heat transfers, and therefore in the duct temperature gradients. (For run 99A typical values of power and flow for fueled driver subassemblies in row 7 are about 500 KWt and 60 gpm; whereas, typical power and flow values in reflector rows 8, 9 and 10 are, respectively, about 15 Kwt and 1.7 gpm, about 10 KWt and 0.76 gpm, and about 5 KWt and 0.62 gpm.) The effect of an assumed 40% reduction in reflector power-to-flow ratio, simulating for example 25% less power and 25% greater flow of the reflector subassemblies for run 99A, would instead tend to the row-wise temperature differentials shown in Table 3. Examinations of the $\Delta T$ values show that both rows 7 and 8 would tend to deflect outward. A strong inward deflection of row 10, which is the last row of reflector before the first row of blanket, would also occur.

Table 3. Intra-Row-Average Effective-$\Delta T$ Radially-Across Subassembly-Ducts for Run 99A Assuming 40% Smaller Power-to-Flow in Reflector Subassemblies

| Axial Location | $\Delta T^a$ in °F for Row | | | | | | | | | | | | | | |
|---|---|---|---|---|---|---|---|---|---|---|---|---|---|---|---|
| | 1 | 2 | 3 | 4 | 5 | 6 | 7 | 8 | 9 | 10 | 11 | 12 | 13 | 14 | 15 |
| Clad Top[b] | 0 | -31 | -6 | -15 | -30 | +21 | +58 | +52 | 0 | -83 | -20 | +76 | +62 | +31 | +13 |
| Core Top | 0 | -15 | -8 | -8 | -20 | +16 | +37 | +31 | 0 | -71 | -6 | +58 | +46 | +23 | +9 |
| Core Midplane | 0 | -6 | -4 | -5 | -10 | +10 | +16 | +5 | -1 | -51 | -3 | +39 | +31 | +15 | +6 |
| Core Bottom | 0 | 0 | 0 | -2 | 0 | +1 | -5 | -13 | -3 | -29 | -1 | +20 | +17 | +8 | +4 |
| $\bar{T}^c$ at Midplane | 49 | 45 | 64 | 64 | 86 | 86 | 67 | 54 | 61 | 69 | 118 | 92 | 58 | 36 | 27 |

a. Positive sign indicates duct temperature larger on side closer to core centerline. (Divide by 1.8 for °C)
b. About 13in (33cm) above core top level. c. Above 700 °F inlet. (371°C)

## CREEP DISTRIBUTIONS

The subassembly-delineated compositions, powers, and flows corresponding to EBR-II run 99A and run 122A form the bases for these calculations. Run 99A is a heterogeneous loading of approximately seven core rows; whereas, run 122A is essentially a homogeneous loading of six core rows. For each of these cases four non-zero distributions (a, b, c, and d) of row dependent values for the creep factors, f, are assumed. The distributions are chosen to simulate creep manifesting itself with time into increasing rows. These are listed in Table 4.

For the subassembly-delineated compositions corresponding to run 99A a modified case assuming 40% reduction in power-to-flow values in the radial-reflector subassemblies is also analyzed.

Table 4. Row-Wise Creep Factors

| 99A Row<br>122A Row | Core<br>1 → 7<br>1 → 6 | Refl.<br>8,9<br>7,8 | Refl.<br>10<br>9,10 | Bkt.<br>11,12<br>11,12 | Bkt.<br>13 → 15<br>13 → 15 |
|---|---|---|---|---|---|
| zero-case | 0 | 0 | 0 | 0 | 0 |
| a-case | 1 | 1/2 | 0 | 0 | 0 |
| b-case | 1 | 1 | 1/2 | 0 | 0 |
| c-case | 1 | 1 | 1 | 1/2 | 0 |
| d-case | 1 | 1 | 1 | 1 | 1/2 |

## RESULTS

The creep-modified row deflections and interactions at zero power for the assumed a, b, c, and d creep distributions are listed in Tables 5, 6, and 7, respectively, for the 99A, 122A, and modified 99A cases. The radial displacements of the rows are given for the near-to-midplane button levels and for the duct tops. Positive values indicate outward displacements and negative values inward displacements from vertical. Asterisks indicate interactions of duct rows.

Table 5. Row-Wise Restrained Radial Duct-Deflections (mils)[a] for Run 99A at Zero Power Resulting from Various Assumed Row-Wise Irradiation-Enhanced Creep Distributions Assuming No Void-Swelling

| | | Row Number | | | | | | | | | | | | | | |
|---|---|---|---|---|---|---|---|---|---|---|---|---|---|---|---|---|
| Case | Duct Axial Loc | 1 | 2 | 3 | 4 | 5 | 6 | 7 | 8 | 9 | 10 | 11 | 12 | 13 | 14 | 15 |
| zero | Top | 0 | 0 | 0 | 0 | 0 | 0 | 0 | 0 | 0 | 0 | 0 | 0 | 0 | 0 | 0 |
| | Button | 0 | 0 | 0 | 0 | 0 | 0 | 0 | 0 | 0 | 0 | 0 | 0 | 0 | 0 | 0 |
| a | Top | 0 | 11 | -1 | -3 | -5 | -14 | -25 | 21 * | -6 | 0 | 0 | 0 | 0 | 0 | 0 |
| | Button | 0 | 1 | 0 | 0 | 0 | -1 | -3 | 1 | -1 | 0 | 0 | 0 | 0 | 0 | 0 |
| b | Top | 0 | 11 | -1 | -3 | -5 | -14 | -25 | 30 * | 3 | 18 | 1 | 0 | 0 | 0 | 0 |
| | Button | 0 | 1 | 0 | 0 | 0 | -1 | -3 | -4 | 6 * | 4 * | 1 | 0 | 0 | 0 | 0 |
| c | Top | 0 | 11 | -1 | -3 | -5 | -14 | -25 | 30 * | 3 | 28 * | 1 * | -26 | 0 | 0 | 0 |
| | Button | 0 | 1 | 0 | 0 | 0 | -1 | -3 | -4 | 6 * | 4 | 4 | 3 * | 0 | 0 | 0 |
| d | Top | 0 | 11 | -1 | -3 | -8 | -20 | -35 | 14 * | -13 | 6 * | -21 * | -48 | -25 | -11 | -1 |
| | Button | 0 | 1 | 0 | 0 | -2 * | -4 * | -8 * | -10 | -3 * | -6 | -3 | 5 * | 2 * | 0 | 0 |

[a]Divide by 39.4 for millimeters.

Table 6. Row-Wise Restrained Radial Duct-Deflections (mils)[a] for Run 122A at Zero Power Resulting from Various Assumed Row-Wise Irradiation-Enhanced Creep Distributions Assuming No Void-Swelling

| Case | Duct Axial Loc | Row Number 1 | 2 | 3 | 4 | 5 | 6 | 7 | 8 | 9 | 10 | 11 | 12 | 13 | 14 | 15 |
|---|---|---|---|---|---|---|---|---|---|---|---|---|---|---|---|---|
| zero | Top | 0 | 0 | 0 | 0 | 0 | 0 | 0 | 0 | 0 | 0 | 0 | 0 | 0 | 0 | 0 |
| | Button | 0 | 0 | 0 | 0 | 0 | 0 | 0 | 0 | 0 | 0 | 0 | 0 | 0 | 0 | 0 |
| a | Top | 0 | -25 | 6 | -6 | -13 | -21 | -47 | 27 | * 0 | 0 | 0 | 0 | 0 | 0 | 0 |
| | Button | 0 | -3 | 1 | 0 | -1 | -2 | -4 | -1 | 0 | 0 | 0 | 0 | 0 | 0 | 0 |
| b | Top | 0 | -25 | 2 | -13 | -26 | -45 | * -72 | 56 | * 29 | 20 | 0 | 0 | 0 | 0 | 0 |
| | Button | 0 | -3 | -1 | * -4 | * -7 | * -12 | 1 | -1 | 4 | 2 | 0 | 0 | 0 | 0 | 0 |
| c | Top | 0 | -25 | 2 | -13 | -26 | -45 | * -72 | 69 | 49 | 40 | * 13 | 0 | 0 | 0 | 0 |
| | Button | 0 | -3 | -1 | * -4 | * -7 | * -12 | 1 | 6 | 4 | 3 | 6 | * 2 | 0 | 0 | 0 |
| d | Top | 0 | -25 | 2 | -13 | -26 | -45 | * -72 | 67 | 44 | 27 | * 0 | 0 | * -27 | -15 | -5 |
| | Button | 0 | -3 | -1 | * -4 | * -7 | * -12 | 1 | 5 | * 1 | * -3 | 16 | 1 | -1 | -1 | 0 |

[a]Divide by 39.4 for millimeters.

Table 7. Row-Wise Restrained Radial Duct-Deflections (mils)[a] for Modified Run 99A[b] at Zero Power Resulting from Various Assumed Row-Wise Irradiation-Enhanced Creep Distributions Assuming No Void-Swelling

| Case | Duct Axial Loc | Row Number 1 | 2 | 3 | 4 | 5 | 6 | 7 | 8 | 9 | 10 | 11 | 12 | 13 | 14 | 15 |
|---|---|---|---|---|---|---|---|---|---|---|---|---|---|---|---|---|
| zero | Top | 0 | 0 | 0 | 0 | 0 | 0 | 0 | 0 | 0 | 0 | 0 | 0 | 0 | 0 | 0 |
| | Button | 0 | 0 | 0 | 0 | 0 | 0 | 0 | 0 | 0 | 0 | 0 | 0 | 0 | 0 | 0 |
| a | Top | 0 | 9 | -5 | -8 | -13 | -32 | * -59 | -33 | -21 | 0 | 0 | 0 | 0 | 0 | 0 |
| | Button | 0 | 1 | 0 | -1 | -1 | * -5 | 0 | -3 | -2 | 0 | 0 | 0 | 0 | 0 | 0 |
| b | Top | 0 | 9 | -5 | -8 | -19 | -38 | * -65 | -67 | -42 | 46 | * 19 | 13 | 9 | 5 | 1 |
| | Button | 0 | 1 | 0 | -1 | * -4 | * -8 | -3 | -6 | -3 | -3 | 9 | * 7 | * 5 | * 3 | * 1 |
| c | Top | 0 | 9 | -5 | -12 | -24 | -45 | * -72 | -76 | -61 | 60 | * 33 | * 6 | 20 | 16 | 11 |
| | Button | 0 | 1 | 0 | -3 | * -6 | * -11 | -7 | * -11 | * -13 | * -15 | 13 | 13 | * 10 | * 8 | * 6 |
| d | Top | 0 | 9 | -7 | -15 | -27 | -49 | * -76 | -81 | -67 | 48 | * 21 | * -6 | -1 | 9 | 14 |
| | Button | 0 | 1 | * -2 | * -4 | * -8 | * -12 | -9 | * -13 | * -15 | * -17 | 7 | 16 | * 12 | * 9 | * 7 |

[a]Divide by 39.4 for millimeters.
[b]Assumes 40% smaller power-to-flow ratios in reflector subassemblies.

The predicted trends of the power-dependent bowing components of the PRDs for the 99A, 122A, and modified 99A cases are shown in Figs. 1, 2, and 3, respectively. Calculated reactivities in units of %Δk/k are converted to inhours (Ih) by the factor 441 Ih per %Δk/k. For conversion to cents divide the inhour values by 3 Ih per ¢, corresponding to $\beta_{eff} = 0.0068$.

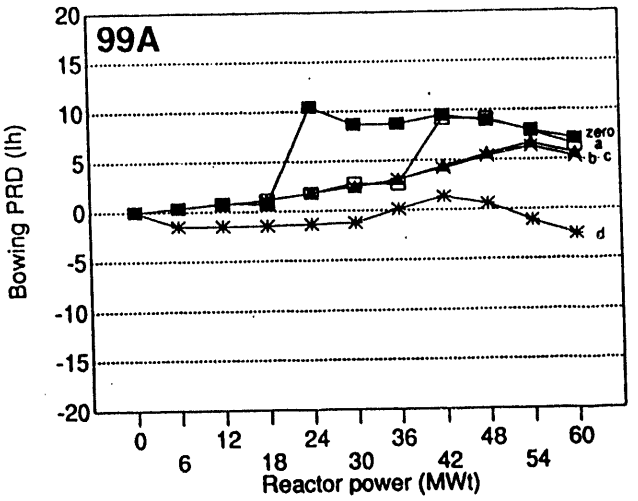


Fig. 1. Trends in bowing reactivity resulting from increasing (a,b,c, and d) irradiation enhanced creep assumptions of reflector and blanket ducts for the run 99A case.

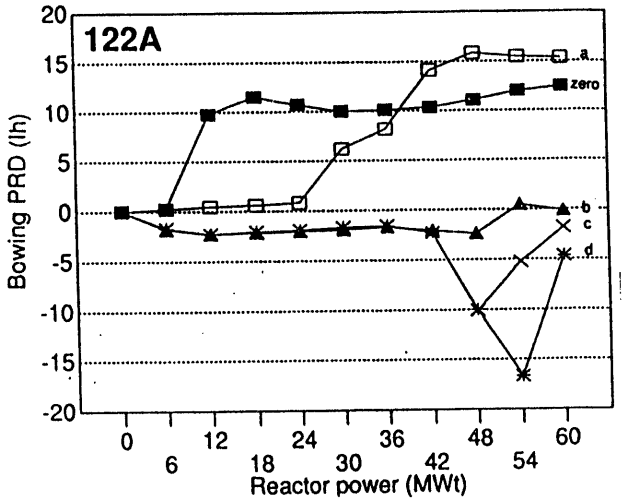


Fig. 2. Trends in bowing reactivity resulting from increasing (a,b,c, and d) irradiation-enhanced creep assumptions of reflector and blanket ducts for the run 122A case.

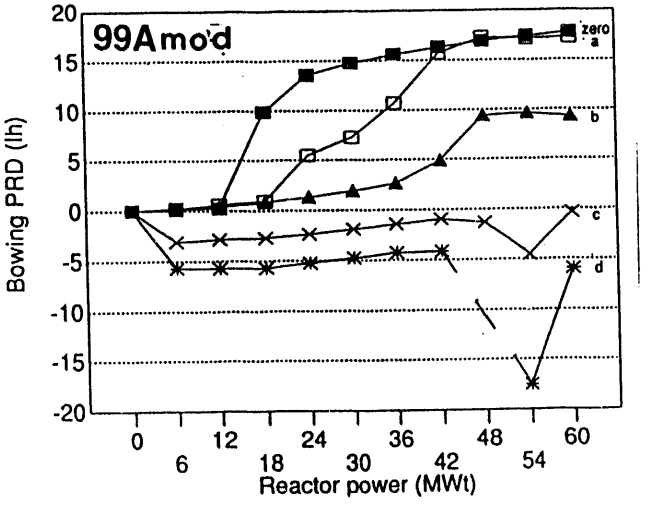


Fig. 3. Trends in bowing reactivity resulting from increasing (a,b,c, and d) irradiation-enhanced creep assumptions of reflector and blanket ducts for the modified run 99A case.

99A

Case zero: The reactivity values are negligible until a rapid positive rise at a power threshold. This is followed by a slowly decreasing plateau. The rapid positive rise results primarily from the thermal bowing interactions at the duct tops of core row 7 and the row 8 reflector row. Row 7 tends to flower outward and row 8 strongly flowers inward. This compresses the core at the button level. The plateau occurs because thermal expansions of the core rows at the button level resist further core compaction and subsequently the core compaction is reduced somewhat by these outward core forces. (Detailed correlations of reactivity and deflections as functions of power are given in Reference 1 for the zero creep situation.)

Case a: The reactivity is essentially a shift of the zero creep case. A larger power fraction must be attained before the tops of rows 7 and 8 interact to rapidly compress the core. This occurs because the assumed creep distribution causes the rows to initially start out with opposite deflections which must be thermally overcome.

Cases b and c: In these cases the curves are very similar and represent cases of extreme shifts so that the rapid positive rise is essentially not attained. Complete creep of row 8 results in the top interacting only at the very high power with row 7 top. These cases represent the lesser positive reactivity transition situation preceding the negative values of reactivity exhibited in the d-case.

Case d: Here the reactivity quickly exhibits a small constant negative value for a large range of power. This results from the core being compressed at zero power because of the additionally strong assumed creeps of the row 11 and 12 blanket subassemblies. Creep causes the residual deflections to be strongly flowered inward. These deflections effect the reflector rows and lead to the initially compressed core. With a relatively small increase in power this compression is relieved because the thermal bowing temperature gradients tend to diminish the inward flowering. The core is quickly relieved of its compression. Essentially nothing subsequently occurs until at high powers either the out-of-core rows by relief of the creep deflections attempt to compress the core if possible, or the thermal expansions of the core rows at button level attempt to expand the core depending on the relative forces.

122A

Case zero: The reactivity values are negligible until a rapid positive rise at a power threshold. This is followed by a plateau. The rapid positive rise results primarily from the thermal bowing interactions at the duct tops of reflector row 7 with the duct tops of reflector row 8. Row 7 strongly flowers outward and row 8 tends to flower inward. This compresses the core at the near-to-midplane button level. The plateau occurs because the resulting interactions of the core rows at the button level resist further core compaction. (Detailed correlations of reactivity and deflections as functions of power are given in Reference 1 for the zero creep situation.)

Case a: The reactivity is essentially a shift of the zero creep case. A larger power fraction must be attained before the top of row 7 interacts with row 8 top to rapidly compress the core. This occurs because the assumed creep distribution causes these rows to initially start out with opposite deflections which must be thermally overcome.

Cases b, c, and d: The curves are very similar over a large power range in that the reactivities quickly exhibit small constant negative values. These result from the core being compressed at zero power because of the stronger assumed creep of the rows 7 and 8 reflector subassemblies. Creep causes

the residual deflections of row 7 to be strongly flowered inward and row 8 outward. These initial deflections of the reflector rows lead to the small initial compression via the inward force through the top of row 7. With a relatively small increase in power this small compression is quickly relieved because the thermal bowing temperature gradients tend to diminish these initial deflections. Essentially nothing subsequently occurs until at higher powers either the out-of-core rows by relief of the creep deflections compress the core if possible, or the thermal expansions of the core rows at button level expand the core depending on the relative forces.

99A (modified)

Case zero: A larger positive reactivity is attained here than in the zero creep normal base case. The core compression by the out-of-core subassembly rows occurs sooner and are larger. Examination of the $\Delta T$ values for the normal base case shown in Table 1 shows that core row 7 has free outward flowering and the row 8 reflector has free inward flowering. In contrast examinations of the $\Delta T$ values of the modified case (shown in Table 3) shows that both rows 7 and 8 free-flower outward. The impetus for strong compression of the core arises from the strong inward flowering of row 10 (which is the last row of reflector before the first row of blanket). This large inward displacement of row 10 top encounters the top of row 9 which in turn encounters the outward flowering of the row 8 top which in turn results in core compression at the button level contacts of row 8 with core row 7.

Case a: The positive reactivity threshold is here shifted toward higher power. This occurs because rows 8 and 9 of reflector are assumed to be partially crept which causes inward flowering at zero power. A larger outward-flowering thermally caused deflection component is then needed to overcome this initial inward flowering. Strong thermal inward top deflection of row 10 must wait for rows 8 and 9 to overcome their partial reverse creeps before encounter occurs.

Case b: Here the positive reactivity shift is toward even larger powers. This results because, in addition to rows 8 and 9 having more creep than in the a-creep assumption, the otherwise strongly inward thermal bowing of row 10 must now first overcome its initial outward bowing because of the assumption of its partial creep. This initial, zero power, deflection is due to the top of row 10 encountering the top of row 11. The row 10 top eventually flowers inward causing core compression and increasing positive reactivity. The latter levels at higher powers because the button level thermal expansions of the core rows tend to expand the core.

Case c: Because of the much larger row 10 creep its initial strong outward top deflection causes button level inward forces which are transmitted via the intervening rows and lead to some core compression at zero power. With power this slight core compression is quickly relieved and the reactivity is a flat negative value. Subsequently with large power values the decreasing reactivity of the delayed core thermal expansion at button levels and the increasing reactivity of delayed compression from row 10 thermal deflections occur.

Case d: This is similar to the c-creep situation except that the strong assumed creep also in the first rows of blanket augments the initial compression of the core. The release of the compression with power exhibits a larger flat negative reactivity. With increasing power the core is essentially neither compressed nor expanded because the thermal effects upon bowings must first overcome the various creep effects. The very large core expansion at high powers occurs because here the interacting core rows are not impeded by the rows external to the core. This is here, however, then reversed with increasing power by the inward-pressing forces of the external rows.

## CONCLUSIONS

For cases 99A and 122A the primary impetus for core compression resulting in a positive bowing reactivity is the strong inward flowering of row 8, which encounters the outward flowering of row 7, at the top. (In contrast for the modified 99A case the primary impetus for core compression is the strong inward flowering of row 10, the last reflector row, whose top forces row 9 top to encounter the outward flowering row 8.) With creep encounters occur at higher powers because the reverse deflections at zero power necessitate first thermally overcoming these reversals. With increased creeps of outer reflector rows and creeps in leading rows of blanket the reverse deflections present at zero power cause initial compressions of the core. With power these compressions are quickly overcome by the thermal gradients so that for a large power range there result essentially constant negative bowing reactivities. At higher powers the constant negative values can be modified by core compressions, if possible, because of the previously described differing top encounters and/or by core self-expansions because of interactions of button-level diametrical thermal expansions of the core ducts.

### Acknowledgements

The author wishes to thank D. A. Kucera for help in carrying out many of these calculations.

This work was supported by the U.S. Department of Energy, Nuclear Energy Programs, under Contract W-31-109-ENG-38.

### REFERENCES

1. D. MENEGHETTI and D. A. KUCERA, "Duct-Bowing Reactivity Trends in EBR-II," Ann. Nucl. Energy, Vol. 21, No. 1 (1994).

2. D. A. KUCERA and D. MOHR, Unpublished, Argonne National Laboratory (1971).

3. D. A. KUCERA and D. MOHR, "Bow-V: A CDC-3600 Program to Calculate the Equilibrium Configurations of a Thermally Bowed Reactor Core," ANL/EBR-014, Argonne National Laboratory (1970).

DATE
FILMED
4/11/94
END